Design of Multifunctional Polymer Nanocomposites Empowered by Predictive Multiscale Modeling

Ying Li · **Zeliang Liu** · **Zheng Jia** · **Wing Kam Liu**

Abstract Polymer nanocomposites have been envisioned as advanced materials for improving the mechanical performance of neat polymers used in aerospace, petrochemical, environment and energy industries. With the filler size approaching the nanoscale, composite materials tend to demonstrate remarkable thermomechanical properties, even with addition of a small amount of fillers. These observations confront the classical composite theories and are usually attributed to the high surface-area-to-volume-ratio of the fillers, which can introduce strong nanoscale interfacial effect and relevant long-range perturbation on polymer chain dynamics. Despite decades of research aimed at understanding interfacial effect and improving the mechanical performance of composite materials, it is not currently possible to accurately predict the mechanical properties of polymer nanocomposites directly from their molecular constituents. This perspective paper will present and discuss a multiscale modeling method for understanding and predicting the macroscopic viscoelasticity of polymer nanocomposites directly from their molecular constituents. This will maximize the computational ability to design novel polymer composites with advanced performance for many industrial applications. Nevertheless, predicting viscoelasticity is a multifaceted challenge, due to a disparate range of mechanisms occurred on multiple spatiotemporal scales. To overcome this challenge, different computational schemes will be used to uncover the key physical mechanisms at the relevant spatial and temporal scales for predicting and tuning constitutive behaviors *in silico*, thereby establishing a bottom-up virtual design principle to achieve unprecedented mechanical performance of nanocomposites. Elucidating the viscoelasticity of polymer nanocomposites through fundamental studies is a critical step to generate an integrated computational material engineering principle for discovering and manufacturing new composites with transformative impact on aerospace, automobile, petrochemical industries.

Keywords Polymer Nanocomposites · Multiscale Modeling · Viscoelasticity · Material Design

Ying Li (✉)
Department of Mechanical Engineering & Institute of Materials Science, University of Connecticut, Storrs, CT 06269, USA
Tel.: +1 860-486-7110
Fax: +1 860-486-5088
E-mail: yingli@engr.uconn.edu

Zeliang Liu
Theoretical and Applied Mechanics, Northwestern University, Evanston, IL 60208, USA
E-mail: zeliangliu2017@u.northwestern.edu

Zheng Jia
Department of Mechanical Engineering, Northwestern University, Evanston, IL 60208, USA
E-mail: zheng.jia@northwestern.edu

Wing Kam Liu (✉)
Department of Mechanical Engineering, Northwestern University, Evanston, IL 60208, USA
Tel.: +1 847-491-7094
Fax: +1 847-491-3915
E-mail: w-liu@northwestern.edu

1 Introduction and Motivation

Polymer nanocomposites (PNCs) have been envisioned as advanced materials for improving the mechanical performance of neat polymers used in aerospace, petrochemical, environment and energy industries [1]. With the filler size approaching the nanoscale, composite materials tend to demonstrate remarkable thermomechanical properties, even with addition of a small amount of fillers [2,3]. These observations confront the classical composite theories and are usually attributed to the high surface-area-to-volume-ratio of the fillers, which can introduce strong interfacial effect and

relevant long-range perturbation on polymer chain dynamics [1,4,5,6,7,8]. As such, the Young's modulus, viscoelasticity, yield stress, fracture toughness and glass transition temperature (T_g) of these materials have been dramatically changed. Despite decades of research aimed at understanding the interfacial effect and improving the mechanical performance of composite materials, it is not currently possible to accurately predict the mechanical behaviors of PNCs directly from their molecular constituents. Therefore, design of PNCs traditionally relies on the slow and in-efficient 'Edisonian' approaches.
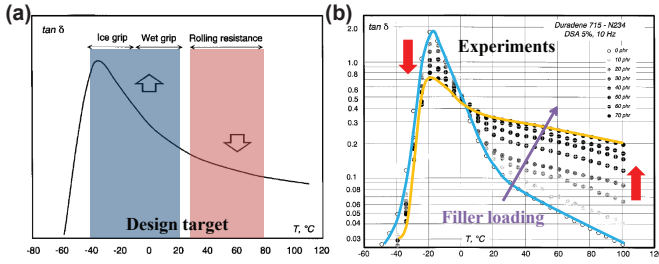

Fig. 1 (a) Design target of $\tan(\delta)$ in tire industry and (b) filler loading effect on $\tan(\delta)$ in synthetic rubber-carbon black composites observed in experiments. Note that $T_g = -67°C$ for rubber materials. These figures are adapted and modified from [9].

Viscoelasticity characterizes the most important mechanical behaviors of PNCs, represented by the storage (elastic) modulus G' and loss (viscous) modulus G''. Their ratio G''/G', so-called $\tan(\delta)$, denotes the energy dissipation during the deformation process. We have $\tan(\delta) = 0$ for a metal spring, indicating that it loses very little energy when it is stretched and let go. However, other materials, like rubber, carbon-black filled rubber, or silica filled rubber, will have larger value of $\tan(\delta)$ due to the molecular and filler-rubber interface motion. In the tire manufacturing and related industry, $\tan(\delta)$ is used as the gold standard in design and evaluation the performance of tire materials [9]. In the temperature range of 40-80 °C, the rolling resistance of tire correlates directly with $\tan(\delta)$: the smaller $\tan(\delta)$, the lower rolling resistance. A higher $\tan(\delta)$ at lower temperatures will lead to good wet grip. It has been recognized that 10% of fuel used in the average car is taken for overcoming the rolling resistance of tires. By itself, the automobile rolling resistance is responsible for astonishing 4% of worldwide carbon dioxide emissions from fossil fuels. Thus, it is another way to improve the fuel economy by lowering the rolling resistance (or $\tan(\delta)$). However, in the tire world, people are constrained tradeoffs in which an improvement to rolling resistance has to sacrifice the wet-road grip and/or durability of tire.

As shown in Fig. 1(a), the value of $\tan(\delta)$ for rubber compounds has to be enlarged and reduced simultaneously at high (40-80 °C) and low (-40-20 °C) temperature ranges, respectively, to reduce the rolling resistance and enhance ice and wet grips. However, for the typical synthetic rubbers filled by carbon blacks, experimental results reveal that $\tan(\delta)$ value will be enlarged and reduced at high and low temperature ranges, respectively, by increasing the loading of carbon blacks (cf. Fig. 1(b)). Therefore, reducing $\tan(\delta)$ at 40-80 °C, however, also reduces the $\tan(\delta)$ at -40-20 °C. This is why the wet-grip and rolling resistance of tires are hard to pull apart. Thus, the manufactured rubber compound cannot satisfy the requirements of tire design for targeted performance. The Transportation Research Board estimates that if tire rolling resistance were reduced by 50%, 10 billion gallons of fuel (7.7% of our total national fuel expenditure) could be saved per year. However, it is currently unknown whether it is possible to design and manufacture the polymer compounds meeting the above requirements. Moreover, the physical mechanisms underpinning the $\tan(\delta)$ change induced by the added fillers are still not clear. These limitations and challenges call for a deep understanding on the viscoelastic properties of PNCs and a useful toolbox for predicting these properties from their molecular constituents.

Constitutive modeling on linear elastic behaviors of PNCs dates back to the advent of micromechanics, initiated by Einstein's [10] and Smallwood's [11] two-phase model. In this model, the fillers are assumed to be spherical and rigid, immersed in an elastic polymer matrix, ignoring the aspect ratio, finite stiffness, and local changes of polymer behaviors near the fillers (interphase). Subsequent micromechanics theories have been developed through phenomenological or mean-field theoretical approaches [12,13,14], by using additional terms to represent these factors. Later on, these theories have been generalized to linear viscoelasticity by using the Fourier transform of the constitutive law, and some of them have explicitly considered the interphase regions in PNCs [15,16,17,18]. Besides, based on these micromechanics models, nonlinear, time-dependent constitutive models have been developed for filled elastomers, such as the Bergström-Boyce model [19,20,21], for finite deformation regime. These theories are relatively easy to use and fast to compute, and the sufficiently advanced ones have good descriptive capabilities and can be calibrated for multiple materials, which makes them useful for modeling and design of devices and components. However, they account for interphase properties in only an approximate way. In some models, the filler is assumed to have no effect on local stress relaxation in the matrix, and in other cases, the effect is prescribed to match particular experimental observations through a fitting procedure. The common shortcoming of all existing methods is that they are based on top-down experimental data that can only be correlated with nanoscale interfacial phenomena in an indirect, case specific fashion. As such, a

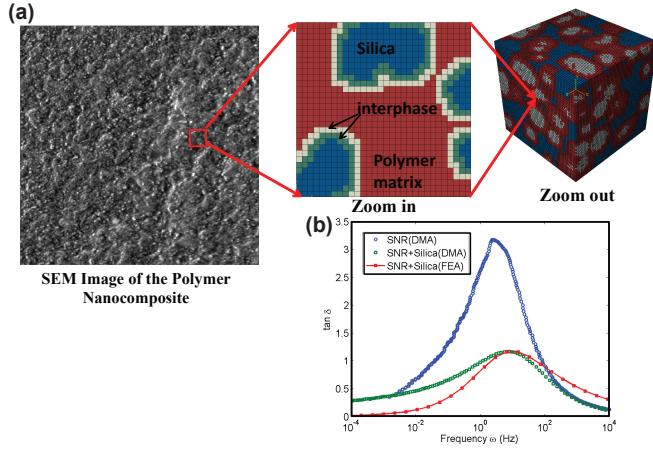predictive modeling capability that is necessary for computational materials design remains to be established.

Fig. 2 (a) Finite element modeling scheme on viscoelasticity of PNCs. (b) Comparison between experimental measurements and simulation results.

The limitations of these models and the increase in available computing power have led us to re-examine the reductionist approach. As a result, one of the most sophisticated methods for modeling PNCs has been developed by Northwestern University in collaboration with Goodyear Tire and Rubber Company (GT), led by the corresponding author of this work, W.K. Liu, and L.C. Brinson, W. Chen, D. Dikin (among others) [22, 23]. First, images of the composite microstructure obtained using scanning electron microscopy (SEM) were binarized and converted into finite element models, and interphase regions were explicitly placed around each filler particle or cluster, as shown for 2D in Fig. 2(a). Reconstructed images created to reproduce the observed filler size, shape, and dispersion statistics were also considered. Afterwards, the 3D representative volume element has been reconstructed through the statistical analysis [24, 25, 26], by accurately reflecting the microstructure information revealed through SEM. Next, the constitutive behavior of the polymer matrix was determined empirically by fitting a standard phenomenological form (Prony series) to experimental results from dynamic mechanical analysis (DMA) of unfilled synthetic natural rubber. Finally, the interphase thickness and deviation from matrix constitutive behavior were then calibrated to best fit DMA results of the composite material, as shown in Fig. 2(b). The difficulty arises from the thickness and properties of interphase region, which is still a debating issue [6, 27, 28, 29, 30, 31, 32]. Therefore, the mechanical behaviors of the interphase regime can only be calibrated from the matrix behavior for fitting the experimental data of PNCs, with predefined interphase thickness [22, 33]. The result modeling scheme is a powerful methodology

with sophisticated descriptive capabilities for microstructure of PNCs. However, it still suffers from the lack of predictive capability, as the interphase properties and thickness are needed to be calibrated for matching experimental data. Nevertheless, the estimated viscoelastic properties ($\tan(\delta)$) of PNCs are still far away from the experimental results in certain regime, as shown in Fig. 2(b).

Essentially, all the above modeling methods are based on the micromechanics theories, which require the mechanical properties of different phases known as *a prior*. Thus, these methods are not particularly suitable for the design of PNCs, as the interphase regimes around the surface of nanoparticles are still not clear [34, 6]. There is an urgent need to develop a predictive multiscale modeling scheme for PNCs, by overcoming the above limitations.

To address the above issue and challenge, the goal of our research here is to create a model that can provide guidance towards the design of materials, which necessitates predictive models of the effects of confinement and the strength of polymer-filler interaction on the resultant macroscopic behavior of PNCs. Such an effort will create a new and efficient design paradigm for the advanced PNCs. To pursue the multiscale modeling goal, a new physics-based constitutive model will be adopted for studying the viscoelasticity of PNCs, with the relevant physical mechanisms considered. Comparing with other phenomenological or micromechanics modeling strategies [22, 35, 36, 37, 38, 38], all the material law parameters in this constitutive model will have physical meanings, which are signatures of polymer chemistry, physics or dynamics. Therefore, parametric materials design concepts can be easily gleaned from the model. Through the multiscale modeling method outlined by this study, we anticipate that the design process for PNCs will be dramatically accelerated. The flexibility of the method allows for rapid computational prototyping and predicting the performance of PNCs *in silico*, providing new physical insights into the interplay between the molecular scale nanoparticle-polymer chain interaction and macroscopic behaviors of PNCs. Moreover, predicting the mechanical properties of PNCs *a priori* is the Holy Grail of material science and engineering, which is also the goal of the Grand Challenge posted by Materials Genome Initiative [39]. The multiscale modeling method could be used to obtain new paradigms for guiding experimental design of novel PNCs with large and small $\tan(\delta)$ values at low and high temperatures, respectively, meeting the requirements of tire materials (cf. Fig. 1(a)) and reducing the daily energy cost of the automobiles.

This work is organized as follow. Section 2 provides historic views on the mechanical behaviors of polymer matrix, microstructure information of PNCs and related interphase behavior. A multiscale modeling tool box has been presented and discussed in Section 3 for designing viscoelasticity of polymer matrix, understanding interphase thickness

and properties, and mechanical homogenization of microstructured PNCs. The perspective about design of multifunctional PNCs through multiscale modeling is discussed in Section 4.

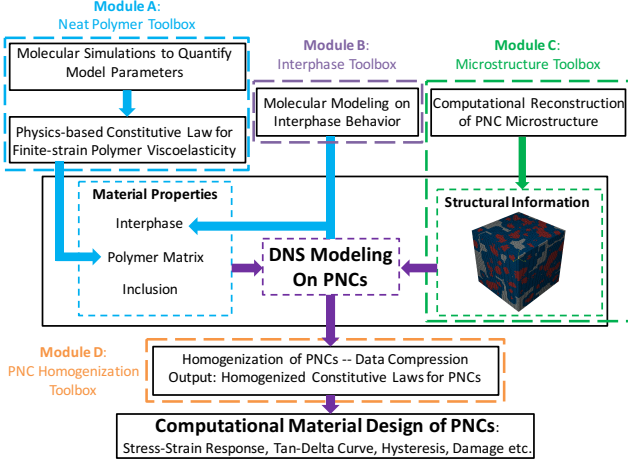## 2 A Predictive Integrated Multiscale Modeling Scheme

Fig. 3 An integrated multiscale modeling scheme to model and predict the mechanical behavior of PNCs by considering material properties and structural information at various lengh scales. The scheme consists of four modules/toolboxes: the neat polymer toolbox, the interphase toolbox, the microstructure toolbox and the PNC Homogenization toolbox

3 Module A: Neat Polymer Toolbox

3.1 Mechanical Behaviors of Polymer Matrix

The prediction of mechanical behaviors of polymeric materials has been an active research area for decades. There have been numerous experimental studies addressing different aspects of the response of elastomers. Experimental evidences have accumulated that polymeric materials exhibit strong rate effects when subjected to dynamic loadings [40], showing a viscoelastic mechanical behavior. It is also well known that the stress in a polymeric specimen relaxes towards an equilibrium state after being subjected to a fixed applied strain [41], which indicates the existence of a hyperelastic strain energy function for very low loading rates. Successful applications of polymeric materials in industry require precise prediction of the complicated mechanical behavior of polymers and thus necessitate the development of accurate constitutive equations.

The macroscopic mechanical response of elastomers originates from their microscopic molecular structure: long randomly oriented polymer chains are joined together via cross-linkers, forming a cross-linked polymeric network; free chains

are randomly distributed within the cross-linked network, as illustrated in Fig. 4(a). Upon loading/unloading, the cross-linked polymeric network is stretched and the free chains diffuse within the network. The cross-linked polymeric network acts as the backbone and is usually capable of recovering its original shapes after unloading, which results in a nonlinear hyperelastic mechanical response. In contrast, reptation of free chains within the cross-linked network is irreversible and causes energy dissipation (i.e. the mechanical response exhibits hysteresis upon cyclic loading), leading to a viscous mechanical behavior. Therefore, to develop a constitutive law that accurately describes the mechanical response of elastomers, their stress response needs to be decomposed into two parts [42,43,44]: a hyperelastic part and a viscous part. Physically, the hyperelastic part is attributed to the nonlinear deformation of the cross-linked polymer network, while the viscous part originates from the diffusion of the free chains.
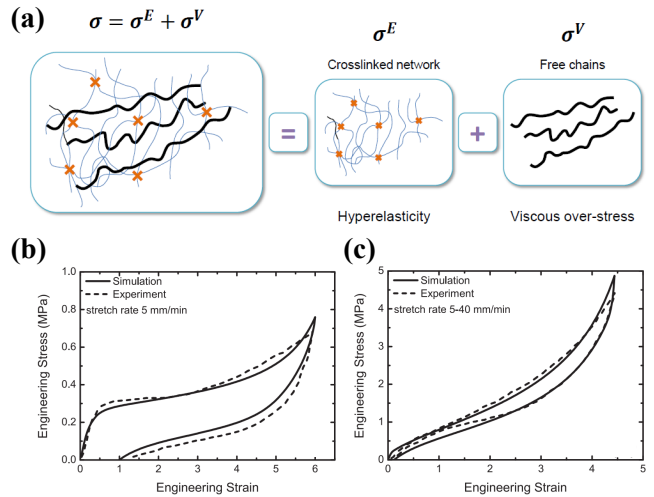

Fig. 4 (a) Microscopic structure of an elastomer can be decomposed into a cross-linked polymer network with free chains. The hyperelastic stress σ^E and viscous stress σ^V are due to the nonlinear deformation of the cross-linked network and diffusion of free chains, respectively. Therefore, the mechanical response of the elastomer can be given as $\sigma = \sigma^E + \sigma^V$. (b) Uniaxial loading and unloading behaviors of unvulcanized NR at room temperature. (c) Uniaxial loading and unloading behaviors of peroxide vulcanized NR at room temperature.

3.1.1 Hyperelasticity of Polymers

The nonlinear elasticity of a cross-linked polymeric network is typically characterized by a hyperelastic constitutive model, which is governed by a strain energy density function W. Depending on the approach followed by the authors to develop the strain energy function W, the hyperelastic models can be classified into phenomenological and physics-based

models. The phenomenological models are mainly obtained from invariant-based continuum mechanics treatment of W and can be used to fit experimentally observed mechanical behaviors. The strain energy density W must depend on stretch via one or more of the three invariants of the Cauchy-Green deformation tensor. Model parameters in phenomenological models usually carry no explicit physical meaning and can only be calibrated by fitting experimental data. Physics-based models are derived based on polymer physics and statistical mechanics which begins by assuming a structure of randomly-oriented long molecular chains. The strain energy density function W for physics-based models depends on the microscopic structure of the polymeric network, in which model parameters are related to the underlying polymer physics/chemistry/dynamics and can be calibrated by using information of the microscopic structure of elastomers. Along this line, the most widely used phenomenological models include but are not limited to the Mooney Model (1940) [45], the Mooney-Rivlin Model (1948) [46], the Ogden Model (1972) [47], the Yeoh Model (1993) [48] and the Gent Model (1996) [49]. An excellent review of the detailed mathematical formulation of aforementioned phenomenological hyperelastic models is given by Marckmann and Verron [50]. For the physics-based models, there are the Neo-Hookean Model (1943) [51], the 3-Chain Model (1942) [52], the Arruda-Boyce (8-Chain) model (1993) [53], the slip-link model (1986) [54], the extended tube model (1999) [55], the non-affine micro-sphere model (2004) [56], and the non-affine network model (2013) [57]. Details about these physics-based models have been summarized and compared by Davidson and Goulbourne [57]. The Neo-Hookean Model, the 3-Chain Model and the Arruda-Boyce Model are widely deployed to characterize the hyperelastic response of elastomers because of the compact mathematical form. However, these models cannot capture the stress softening behavior observed in elastomers with low cross-linking density since they ignore the effect of polymer entanglements [57]. The extended tube model and the non-affine microsphere model can capture the stress softening but contains some parameters without clear physical connections or hard to be calculated [57]. Slip-link model and the non-affine network model can capture the stress softening and all their material parameters are connected to molecular quantities. It is worth noting that the non-affine network model is mathematically compact compared to the slip-link model, which facilitates its application in capturing stress-stretch response of elastomers[44].

3.1.2 Viscoelasticity of Polymers

Besides efforts on developing constitutive models to address the equilibrium response (i.e. hyperelasticity) of elastomers, there also exists many models that attempt to address the observed rate dependence. To investigate the finite-strain vis-

coelastic properties of unfilled or filled elastomers, phenomenological viscoelastic constitutive models have been developed by Simo (1987) [58]; Govindjee and Simo (1992) [59]; Lion (1996) [60]; Lubliner (1985) [61]; Keck and Miehe (1997) [62] based on stress/strain variables. These phenomenological constitutive models are mainly used to fit existing experiment data since microscopic details about the underlying physics are not considered in the formulation of the constitutive models. Moreover, most of these reported models only capture a subset of the experimentally observed phenomena. In an attempt to overcome the disadvantage of the phenomenological models, Le Tallec et al. (1993) [63]; Govindjee and Reese (1997) [64]; Bergström and Boyce (1998) [65]; Miehe and Göktepe (2005) [66] have developed their constitutive models for finite-strain viscoelasticity based on the tube model developed by Doi and Edwards (1986) [67]. However, these models still have several internal variables or model parameters without any physical significance, and thus have to be classified as micromechanism-inspired phenomenological models. In the information age, computationally understanding or designing materials, as suggested by Materials Genome Initiative (MGI) [39], requires the development of fully physics-based constitutive models with all model parameters related to the molecular physical structure. The aforementioned viscoelastic constitutive models apparently do not meet this requirement.

3.2 Physics-based Constitutive Modeling on Polymer Viscoelasticity

Polymeric materials are characterized by a disparate range of spatial and temporal scales. For instance, the typical covalent bond vibrations are on the length scale of Å and time scale of sub-picoseconds. The typical size of a monomer is a nanometer with relevant dynamics in tens of picoseconds. The overall size of a single polymer chain is represented by its radius of gyration, usually between 10 and 100 nanometers. Depending on its surrounding environments, the relaxation of the single chain lasts about 10 to 100 nanoseconds, but often longer. Beyond a critical concentration, different polymer chains are coiled together with mutual uncrossability. A typical polymeric network has a size of about 1 to 100 micrometers, with a relaxation time on the order of microseconds to milliseconds. Composed of these coils and networks, the bulk polymeric materials are on the length sale of millimeters to centimeters. The relaxation and aging of these materials occur in the range of seconds, hours, days and even years. These multiple, disparate spatio-temporal scales and their interdependence among each other in terms of system behavior (i.e., bulk behavior depends on the behavior of individual polymer chains, and so forth) make it necessary to adopt a multiscale modeling technique that can correctly characterize the hierarchy of scales [43,68], if we

wish to link molecular constituents with macroscopic viscoelastic properties for polymeric materials. To this end, different simulation techniques have to be used to understand these relevant physical mechanisms in the corresponding temporal and spatial scales. More importantly, a bottom-up approach should be created to systematically link these different scales together for establishing a truly multiscale modeling method for predicting the viscoelasticity of polymers.

Recently, Li and Tang [43, 44] have developed a physics-based constitutive model by combining the non-affine network model [57] for hyperelasticity and a modified tube model for viscosity. All the parameters in this constitutive model carry physical significance and the model is able to capture the mechanical response of a wide range of elastomers reasonably well. Specifically, in the constitutive model, the stress response is decomposed into two parts:

$$\sigma = \sigma^E + \sigma^V \tag{1}$$

where σ^E denotes the stress stems from hyperelasticity and σ^V the stress due to viscosity. The non-affine network model yields that σ^E equals to

$$\sigma^E = \frac{1}{J} \sum_{k=1}^{3} \lambda_k \frac{\partial}{\partial \lambda_k} [\frac{1}{6} G_c I_1 - G_c \lambda_{max}^2 ln(3\lambda_{max}^2 - I_1) + G_e \sum_{j=1}^{3} (\lambda_j + \frac{1}{\lambda_j})] v_k \otimes v_k \tag{2}$$

where $\lambda_k (k = 1, 2, 3)$ is the k_{th} principal stretch, J is the Jacobian of deformation gradient tensor F, I_1 is the first invariant of Cauchy-Green deformation tensor and v_k is the k_{th} eigenvector of Cauchy-Green deformation tensor. There are three materials parameters related to the hyperelastic stress and they all carry significant physical meanings: λ_{max} is the maximum extensibility of chains for the hyperelastic part; G_c is the cross-linking modulus of the cross-linked network; and G_e is the entanglement modulus of the cross-linked network. All these parameters can be directly related to the microstructure of cross-linked network [44], which are signatures of polymer chemistry and physics.

As we discussed before, the viscous stress originates from the diffusive behavior of free chains within the elastomer. According to the tube concept pioneered by Doi and Edwards [67], the lateral movement of the free chains is constrained within a tube-like region due to the entanglements with its neighboring chains. As a result, the chains can only move along the central line of the tube by Brownian motion. The central line is the so-called 'primitive chain', defined as the shortest path connecting two ends of the polymer chain upon respecting uncrossability of surrounding chains. Under macroscopic loading, both the cross-linked network and free chains deform accordingly. The primitive chain deforms accordingly: the contour length of the primitive chain and the

unit vector at an infinitesimal segment of the primitive chain are denoted by L_{pp0} and v_0 respectively in the reference configuration; in the current configuration, the primitive chain deforms with contour length and the unit vector denoted as L_{pp} and v. The mathematical formulation of σ^V is based on the configuration of the primitive chain, which is given as

$$\sigma^V = \frac{3k_B T n_v}{n_v b^2} \langle L_{pp} \rangle^2 \sum_{p=1,3,5...}^{\infty} \int_0^t \frac{8}{\pi^2 \tau_d} [-\frac{\partial}{\partial x} E_{\alpha,1}(-x^\alpha)]_{x=p^2(t-t')/\tau_d} \Lambda(t,t') \tag{3}$$

where k_b is the Boltzmann constant, T is the temperature. Moreover, $\langle L_{pp} \rangle$ is the expectation of primitive chain length in the current configuration and $\langle L_{pp} \rangle = \frac{\langle L_{pp0} \rangle}{4\pi} \int_{s2} \|F \cdot v_0\| d^2 v_0$, where $\int_{s2} *dv_0$ represents an integration over all possible orientation of v_0 (i.e. over a unit sphere). $E_{\alpha,1} = \sum_{k=0}^{\infty} x^k / (\alpha k)!$ is the Mittag-Leffler function. $\Lambda(t,t')$ is $\int_{s2} v \otimes v d^2 v \int_{s2} \frac{1}{4\pi} \delta(v - \frac{F(t,t') \cdot v_0}{\|F(t,t') \cdot v_0\|}) d^2 v_0 - \frac{1}{3} I$. Here $\delta(x)$ is the Dirac delta function and I is the identity tensor. The viscous stress σ^V exhibits 6 material parameters: the number of free chains per unit volume: the polymerization degree of free chains n_v, the Kuhn length for the free chains b, the fractional order parameter for the relaxation of free chains α and the disentanglement time for the free chains τ_d, with explicit physical meanings. In contrast to most existing finite-strain viscoelastic model for elastomers, all of the 9 material parameters in this constitutive model carry physical significance and thus each parameter can be directly obtained through molecular dynamics simulations or measured by experiments [43, 68, 44]. This enables a bottom-up approach to predict and design the macroscopic mechanical behavior of an elastomer from its molecular structure, enabling a multiscale simulation methodology to investigate the viscoelastic material behavior of elastomers [43]. The applicability of this model to predict the finite-strain viscoelastic mechanical behavior of real elastomers are demonstrated in Fig. 4(b) and Fig. 4(c) for un-vulcanized polymer and vulcanized polymer, respectively. Comparison between modelling results and experimental measurements indicates that the constitutive model can reasonably reproduce the experimentally observed stress-strain behaviors of vulcanized and un-vulcanized natural rubbers [43, 44]. Moreover, the storage and loss moduli, viscosity, and relaxation modulus for polyisoprene and polyethylene can also be directly predicted by this constitutive model, with corresponding material law parameters determined through large scale molecular simulations [43].

To this end, because of its merits such as physics-based nature and accuracy in capturing finite-strain viscoelastic behavior, the newly developed finite-strain viscoelastic model together with the material parameters calibrated from molecular dynamics simulations can be used to model the mechanical behavior of polymer matrix in PNCs.

4 Module B: Interface Toolbox

4.1 Interphase Behaviors in PNCs

In PNCs, regions with altered mechanical properties are broadly called the *interphase*, and the proximity of polymer chains to solid interfaces, and thus the possibility of their interaction (either through physical or chemical interaction), is termed *confinement*. The key challenge in predicting the performance of a PNC is to quantify the spatially varying changes in interphase constitutive behavior resulting from polymer confinement and controlled by polymer-filler interaction, as a function of filler volume fraction and distribution morphology. Key insight into interphase formation and confinement effects in PNCs has come from studies on polymer thin films supported on solid substrates [69, 70, 71, 72, 73]. In these thin films, both the free surface at the top surface of the film and the solid supporting layer cause extremely complex changes in the behavior of the polymer.

The range and magnitude of these effects have been singled out recently by systematically varying the boundary conditions (free standing film, supported thin film, and polymer layer confined between two surfaces) and surface/polymer chemistry. Most importantly, the Schadler group [74, 75], as well as the Torkelson group [70, 76], have shown a quantitative equivalence between PNCs and polymer thin films with regards to glass-transition temperature (T_g) via the calculation of an equivalent metric of confinement within the nanocomposite from the distribution of filler surface-to-surface distances. Glass transition is a phenomenon inextricably linked to the constitutive (stress-strain) behavior of polymers. A non-crystallizing polymer exhibits rubbery behavior above T_g, while it behaves like a glass below T_g, with the difference between these states characterized by the dynamics and magnitude of stress relaxation. By measuring the glass transition temperature (T_g), it has been shown that the thickness of interphase in a polystyrene film is around several tens of nanometers [69]. Therefore, as the size of the fillers approaches nanoscale, the overall properties of the PNCs will depend a lot on the interphase behaviors. This finding is important because it allows for direct prediction of the of the nanocomposite directly from thin film measurements and microstructural statistics, leveraging current capabilities in accurate computational/experimental characterization of film properties. However, it is currently unknown whether the thin-film analogy can be extended into the constitutive behavior of PNCs, most importantly the stress relaxation behavior of the polymer matrix that governs viscoelastic behavior.

Except the T_g measurements, Cheng et al. measured the mechanical properties of confined polymer films adjacent to a plane substrate through atomic force microscopy (AFM)-based indentation [71]. Two sets of polymer/substrate systems are investigated in their work: PMMA on slica and alumina plates. For both systems, gradients of mechanical properties are observed in interphase regions away from the substrates. Characterized by the modulus, the thickness of the interphase region is around 100nm, and the maximum modulus is on the material interphaes with about 50% increase from bulk PMMA's modulus. An improved understanding of interface and interphase effects in PNCs and polymer thin films, combined with mechanistic approaches to linking polymer chemistry and confinement to relaxation metrics will pave the way for rational materials design using predictive simulations.

4.2 Molecular Modeling on Interphase Behavior

It is well-known that the viscoelasticity of polymers origins from the chain dynamics [77, 78, 67, 79]. For short, oligomer chains, their dynamics is governed by the monomeric friction, which can be described by the classical Rouse model [77]. However, when the polymerization degree N of the chain has been increased beyond the entanglement length N_e, the dynamics of chains will be hindered due to the chain connectivity and uncrossability. These topological constraints are termed as entanglements. These entanglements are commonly assumed to effectively restrict the lateral motion of individual chains into a tube-like regime, pioneered by de Gennes [78] and Doi-Edwards [67]. The so-called tube model has been developed to understand and predict the viscoelasticity of polymers, which has been considered to be the most successful theory in polymer physics in the last three decades. In the tube model, the chain moves in a one-dimensional diffusive behavior, due to the lateral confinement introduced by the entanglements. Thus, the chain can only move back and forth, or reptate, along the central axial of the tube, which is defined as the primitive path (PP). The chain can be considered to be fully relaxed when it escapes the original tube and forms another new one with neighboring chains. The critical time for the chain completely leaves its original tube is defined as the disentangle time, τ_d. When the nanoparticles are added into the polymer network, additional constraints are introduced on the polymer chain dynamics. Consequently, the underlying entanglement network and chain relaxation can be dramatically changed by these nanoparticles, firstly observed by the authors' large scale molecular simulations [4]. Subsequently, both molecular simulations done by Grest and co-workers [80, 81], and theoretical studies done by Schweizer and co-workers [82, 83] have confirmed these observations. Thus, the changes of viscoelasticity of PNCs, comparing with the neat polymers, are induced by the changes of chain dynamics in PNCs [84, 5]. It has been reached agreement that the polymer chain entanglements will be reduced upon adding nanoparticles [4, 80, 81]. However, it is still not clear how the reptation behavior

of polymer chains will be affected by the added fillers. Here we *hypothesize* that the viscoelasticity of PNCs can be accurately understood by fully elucidating the polymer chain dynamics in PNCs.
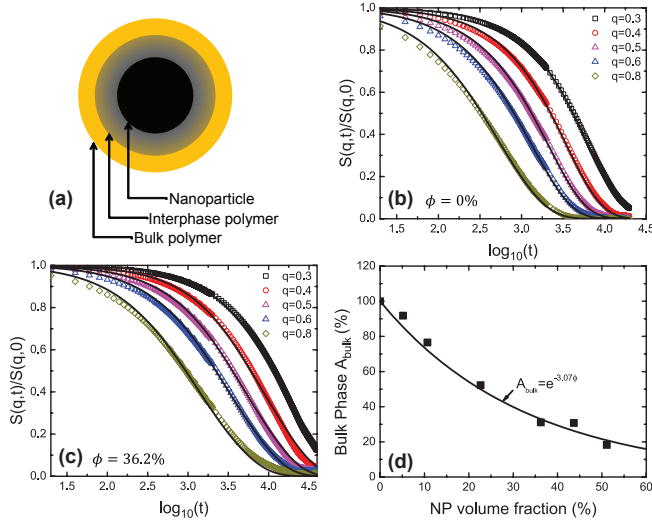

Fig. 5 Molecular simulation on interphase behavior of PNCs. (a) Proposed two layer model for interphase zone in PNC. (b) and (c) represent the dynamic structure factor results for PNCs with nanoparticle volume fractions $\phi = 0\%$ and 36.2%, respectively. (d) denotes the relationship between the bulk phase A_{bulk} and nanoparticle volume fraction ϕ in PNCs. The solid lines in (b) and (c) are fitted by the classical Rouse model and proposed two layer model in (a), respectively.

To further understand the interphase behavior in PNCs, we have carried out large scale molecular dynamics (MD) simulations [6]. Due to the limitation of approachable time scale in MD simulations, only short and unentangled polymer chains are considered. Then, spherical nanoparticles with different volume fractions ϕ are infused into the polymer matrix. The dynamics of polymer matrix has been characterized by the coherent scattering function $S(q,t)$, which is defined as $S(q,t) = 1/N \sum_{i,j} \langle \exp\{i\mathbf{q}[\mathbf{r}_i(t) - \mathbf{r}_j(0)]\}\rangle$. Here $\mathbf{r}_i(t)$ and $\mathbf{r}_j(t)$ represent the positions of monomer i and j at the time t, respectively. The average $\langle * \rangle$ indicates an average over many starting states ($t = 0$) as well as orientations of the scattering vector $\mathbf{q}$. The scattering function $S(q,t)$ cannot only be quantified through the MD simulations [4, 6], but also measured through neutron spin echo experiments [85, 86]. Thus, $S(q,t)$ can be used to directly characterize the dynamics of chains in PNCs for interpreting their viscoelastic properties.

For neat polymers, $S(q,t)$ of short, unentangled chains can be theoretically predicted through the classical Rouse model [77], according to the monomer friction coefficient ζ. Thus, the value of ζ for neat polymer chains can be calibrated through the MD simulation results on $S(q,t)$. When the nanoparticles are added into the polymer matrix, they

dynamics will be altered due to the geometric constraints applied. To understand the dynamics of chains in PNCs, we hypothesize that the $S(q,t)$ can be decomposed into two parts: one is the bulk state and the other is the interphase state, as illustrated in Fig. 5(a). Then, the $S(q,t)$ can be written as $S(q,t) = A_{\text{bulk}}S_{\text{bulk}}(q,t) + A_{\text{conf}}S_{\text{conf}}(q,t)$, where A_{bulk} and A_{conf} denote the fraction of bulk and interphase states, respectively. Thus, $A_{\text{conf}} = 1 - A_{\text{bulk}}$. Here we assume that a fraction of A_{bulk} is far away from the nanoparticle surface and its dynamics is unaffected by the nanoparticle (cf. Fig. 5(a)). While the fraction A_{conf} is located between the bulk phase and nanoparticle with a different relaxation rate or friction coefficient ζ_{conf}, as given in Fig. 5(a). By knowing the monomer friction coefficient ζ from neat polymer, there are only two unknown parameters A_{conf} and ζ_{conf}, which can be fitted through the $S(q,t)$ from MD simulations. As shown in Figs. 5(b)-(c), the $S(q,t)$ for neat polymers and PNCs with $\phi = 36.2\%$ can be well described by the Rouse model and our proposed two layer model, respectively. Moreover, by varying the volume fraction ϕ of nanoparticle, the bulk phase fraction A_{bulk} has been found to be related to ϕ as $A_{\text{bulk}} = \exp(-3.07\phi)$, shown in Fig. 5(d). At the same time, the monomer friction coefficient ζ_{conf} in the interphase region is obtained, which can be related to the viscoelastic properties of interphase through the Rouse model [87]. Therefore, both the volume fraction (thickness) and mechanical properties of interphase region can be directly probed through these MD simulations.

However, the above study is limited to the short and unentangled polymer matrix. When the high entangled chains are confined by nanoparticles, their topological and dynamic properties can be dramatically altered, evidenced by the large scale molecular simulations [4, 5] and experimental observations [85, 86]. However, it still not clear how the reptation of chains will be affected. The viscoelasticity of neat polymers (G' and G'') scales with the loading frequency, following the combine tube relaxation, contour length fluctuation and constraint release effects [79]. These scaling behaviors have been substantially changed due to the added nanoparticles. A rigorous link between the polymer chain dynamics in PNCs and their viscoelastic behaviors will provide detailed explanations on these scaling laws.

5 Module C: Microstructure Toolbox

5.1 Microstructural Information of PNCs

Microstructural information plays an essential role in assessing the effective properties of PNCs [7, 8]. In order to capture the homogenized behaviors of a real material, a 3-dimensional structure needs to be prepared for computational multiscale modeling (e.g. FEM). The start point is always microstructure characterization through experiments;

however, obtaining 3D microstructural information directly from experiments is still burdensome even with the state-of-the-art imaging techniques, especially for soft materials like PNCs [88, 25]. Thus, a myriad of reconstruction techniques which computationally generate 3D microstructures based on 2D images [89, 90, 91, 92, 25] are developed to reduce the complexity and cost in the experimental stage.

Various imaging techniques can be utilized for the microstructure characterization of PNCs. The most common ones are known as SEM and transmission electron microscopy (TEM)[93], both of which are belong to 2D imaging techniques and can only observe the surface or the projection of a thin layer of a material sample. Direct 3D imaging techniques such as X-ray scattering and transmission electron microscopy tomography (TEMT) [94] are not sensitive to the microstructural conformation in the scanning direction, so that they are not capable of providing a 3D image at the RVE scale for polymer nanocomposite where complex filler network are present. According to the authors' knowledge, the state-of-the-art 3D imaging technique at the RVE scale for PNCs is to serial section the 3D material and image each cross-section/layer using standard SEM or TEM. However, besides specific difficulties in serial sectioning soft materials [95], measuring in such a layer-by-layer manner is also extremely time-consuming and expensive since a high spatial resolution in the thickness direction is usually required for characterizing PNCs.
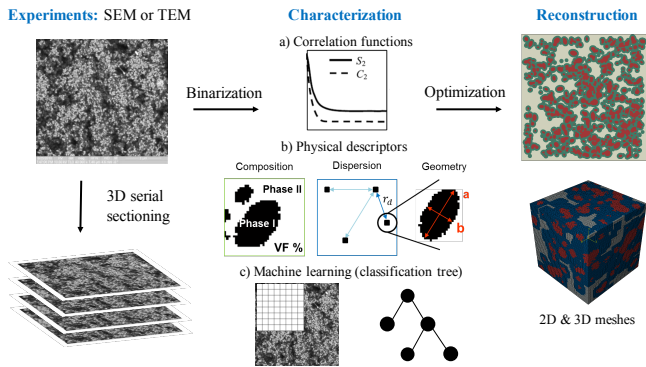

Fig. 6 Characterization and computational reconstruction of PNCs. (a) Various correlation functions are utilized to characterize the microstructure, such as two-point correlation function S_2 and two-point cluster correlation function C_2. (b) Physical descriptors are utilized to describe the microstructure. In [25], physical descriptors are classified into three categories (composition, dispersion and geometry). (c) Machine-learning methods are used to fit a model to microstructural data.

Other than characterizations purely based on experiments, a more efficient way is to computationally reconstruct 3D microstructure based on 2D images from SEM or TEM as shown in Fig.6. By assuming the isotropicity of the 3D mi-

crostructure, a 2D image at the RVE scale would contain all the geometrical features in 3D, and theoretically no microstructural information is missing in the 2D image. In the last two decades, there has been a spectrum of reconstruction approaches, which mainly fall into three basic categories. The first category is based on N-point correlation functions, which mathematically can characterize arbitrary microstructure [89]. Various strategies are utilized to match the correlation functions of the real material sample and reconstructed ones, such as pixel/voxel moving [96], Gaussian random field-based approach [97], support vector machines [90] and generic algorithm [98]. Since correlation functions do not have clear physical meanings, a 2-point correlation function is usually not enough to capture complex microstructures and increasing the dimension of the correlation function becomes a necessary. However, evaluating and integrating higher-dimensional correlation functions are very time-consuming, making it inconvenient to use correlation functions as the design variables. The second category of reconstruction approaches is based on physical descriptors, such as filler volume fraction, the aspect ratio of fillers and nearest neighbor distance [91, 92, 25]. There are mainly two challenges for descriptor-based approaches: 1) finding the most important descriptors to keep the low dimensionality of microstructural characteristics; 2) predicting 3D descriptors from 2D descriptors. The last category of approaches utilizes supervised learning models and does not need predefined characteristics (e.g. correlation functions and physical descriptors). Bostanabad et al. fit a classification tree to the digitized microstructure image and efficiently reconstruct any number of statistically equivalent samples with the same learning model [99]. Although the current work based on supervised learning models is still restricted to 2D reconstruction due to a lack of good 2D-to-3D mapping algorithms, the methodology is general and shows great potential of making the reconstruction much more computationally efficient.

6 Module D: PNC Homogenization Toolbox

6.1 Homogenization of PNCs

Considerable effort has been put into the multiscale modeling of PNCs. Generally, the inputs of these multiscale models are 1) microstructures obtained from imaging techniques or computational reconstructions and 2) material properties of each individual constituents in the PNC. On the other hand, outputs of the models are the macroscopic material properties, such as effective storage and loss moduli. In a multiscale perspective, the developed model links microscopic information to macroscopic material behaviors, which can be further served as a homogenized constitutive relation for macroscopic simulations. Accuracy and efficiency

are two critical aspects for such models; however, it is still challenging for current methods to achieve both aspects at the same time.
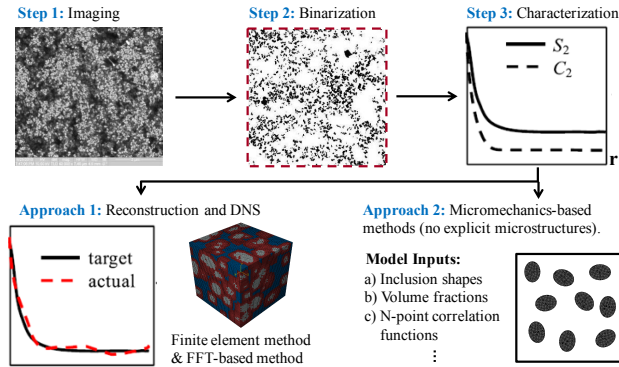

Fig. 7 Basic framework of material characterization and related homogenization of PNCs. (r : distance between a pair of points in the material; S_2 : two-point correlation; C_2 : two-point cluster correlation. 'target' refers to the desired correlation function while 'actual' refers to the one of a reconstructed RVE.) Approach 1 includes DNS methods, such as FEM and FFT-based method. Approach 2 includes various micromechanics-based methods, where the inputs are microstructural descriptors as listed.

Direct Numerical Simulation (DNS) is the most accurate and flexible homogenization method, e.g. Finite Element Method (FEM) [100, 101] and Fast Fourier Transformation (FFT)-based method [102]. For both FEM and FFT-based method, a mesh of the microstructure is needed to start the calculation as shown in Fig.7. FFT-based methods usually require less computational resources than FEM due to its iterative manner and the high efficiency of existing FFT algorithms; However, the mesh in FFT-based method must be uniform and its convergence will be deteriorated if one material phase becomes much stiffer than the other ones. Qiao et al. [103] developed a finite element (FE) model to study the influence of the interphase percolation (overlapping) and gradients on the viscoelastic response of polymer composites. Peng et al. [104] used a FE model to analyze the effects of particle clustering and geometries of nanoparticles on the effective elastic properties of nanocomposite. Their simulations are performed at the scale of a representative-volume-element (RVE), so that the FE models are large enough to statistically represent the heterogeneous composite material. However, simulations at the RVE scale can be computationally expensive especially when the resolution of the FE mesh is high. In order to reduce the cost of each individual simulations, Yin et al. [105] introduced a concept of statistical-volume-element (SVE), wherein the effective responses are obtained by averaging the results of several small SVEs. However, since the SVE scale is be-

low the RVE scale, properties of realizations on the SVE scale depend on the boundary conditions and are prone to oscillation with respect to different microstructures. As a result, a large number of SVEs are usually required to narrow the variance. Such high computational cost makes DNS prohibitive for real-world multiscale engineering problems. Therefore, several approaches have been proposed to improve the efficiency of the prediction without losing substantial accuracy.

For linear viscoelastic properties of polymer composite with perfectly bonded interface, the analysis in the frequency domain becomes equivalent to a linear elastic one [106], so that various micromechanics methods can be applied. As shown in Fig.7, micromechanics methods don't need an explicit mesh of the microstructure which is a must for aforementioned DNS methods, so that burdens from computational reconstructions can be overcome. The microstructure is usually characterized by several microstructural descriptors which will be further incorporated into micromechanics models. On the other hand, since micromechanics methods usually have analytical or semi-analytical solutions based on certain assumptions in the homogenization, they are usually much more efficient than DNS methods. As the first category of micromechanics methods, Hashin and Shrikman gave the upper and lower bounds for the effective properties based on variational principles [107, 108], which only depends on the volume fraction of the inclusion but ignores other key factors, such as inclusion shapes and distributions. Torquato further narrow the bounds by considering higher-order correlation functions of the microstructure [109]. The second category of the micromechanics methods methods starts with the pioneering work of Eshelby [110], which shows that the stress field is constant within an ellipsoidal inclusion embedded in an infinite matrix. Several mean-field approaches were proposed based on Eshelby's solution, such as the Mori-Tanaka method [111] and the self-consistent methods [112]. To consider arbitrary inclusion shape and strain distribution in the inclusion, Liu et al. [36] developed a self-consistent micromechanics method based on a volume integral method. As mentioned before, these theories can be generalized for use with linear viscoelasticity of polymer composite by performing the Fourier transformation of the constitutive law. Liu et al. [113] used the Mori-Tanaka method to evaluate the reinforcing efficiency of inclusions on the storage and loss moduli in polymer nanocomposite. Diani et al. [114] used the 3-phase and 4-phase self-consistent methods to investigate the role of interphase in the carbon-black filled styrene butadiene rubbers.

Recently, Liu et al. proposed a mechanistic and data-driven approach called "self-consistent clustering analysis" (SCA) for homogenizing elastic, viscoelastic and plastic heterogeneous materials [115]. By incorporating data compression algorithms (e.g. k-means clustering) in the offline (or
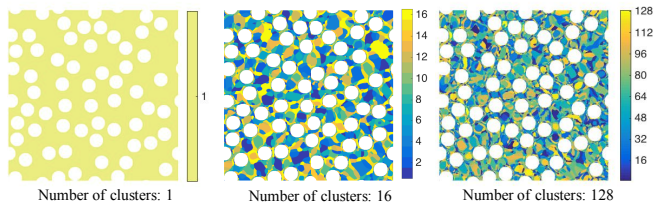
Number of clusters: 1 Number of clusters: 16 Number of clusters: 128

Fig. 8 Clustering results in the matrix of a 2D composite with 1, 16 and 128 clusters. The mesh size of the original DNS is 600×600, and a set of DNS under 3 orthogonal loading conditions (or 6 in 3D) is needed for constructing the database in the offline stage [115].

training) stage, material points with similar mechanical behaviors are grouped into clusters, so that the number of degree-of-freedoms (DOF) in the online (or predicting) stage can be greatly reduced. Clustering results based upon the elastic strain concentration tensor in a 2D composite are provided in Figure 8, and this data compression approach can be applied to both 2D and 3D heterogeneous materials with arbitrary microstructures, such as clusters of nanoparticles and interacting interphases in PNCs. In the online stage, the homogenization of each material cluster is achieved by solving the Lippmann-Schwinger equation self-consistently. For elastic properties, using the same database built on a certain selection of phase properties in the offline stage, SCA predicts the effective properties of new materials with different selections of phase properties accurately with only a small number of clusters, so it is much more efficient than a full-field DNS. Moreover, it also shows great potential of modeling inelastic material behaviors in PNCs, such as the Payne effect.

7 Perspective and Future Works

Computational methods that could facilitate accurate predictions of PNCs can speed up materials design processes aimed at achieving particular viscoelastic properties. PNCs are ubiquitously used in engineering materials ranging from tire to structural materials used in the built environment and aerospace structures. By improving dynamic mechanical performance of these materials, it will be possible to create materials with highly-tunable, predictable relaxation properties. Advances in materials discovery using computation has now become a national priority because it is now known that the slow nature of the materials development process will become the central bottleneck in the way of technological innovation in the near future. In additional to these anticipated societal benefits, fundamental research on PNCs provides unique opportunities to generate impact by integrating new physical concepts into the mechanics of composites. In conclusion, understanding and designing PNCs with unprecedented mechanical properties via multiscale simu-

lation is an emerging and exciting research field. Among a variety list of potentially intriguing directions for future research, several areas present particularly pressing needs.

(i) Physically understanding on the material behaviors of the interface between nanoparticle and polymer matrix in PNCs is one of the holy grail in polymer science. It is critical to develop new experimental techniques to characterize and quantitatively measure the mechanical and topological properties of the interphase region, such as the variation of polymer chain dynamics and interphase thickness, which are not accessible by existing experimental tools. Moreover, the computational methods, such as molecular dynamics, can be applied to understand the structure and dynamic properties of chains in vicinity of nanoparticles, as shown in Section 3.2. However, further studies on high entangled chains are still beyond the capability of current methods, as the relaxation time of the chain $\tau_d \sim N^3$, where N is the polymerization degree. Therefore, the corresponding simulations need multiple years to finish, given by the current state-of-the art supercomputers. Development of more advanced computational method could benefit the fundamental understandings on the interfacial properties in PNCs through large scale computation.

(ii) The development of new physics-based viscoelastic models for PNCs with all model parameters connected to molecular structures is highly desired. In this work, we have introduced an newly developed physics-based viscoelastic constitutive model for polymer matrix. However, the key challenges and opportunities reside in the fact that the model cannot capture the influence of nanofiller on the mechanical response of PNCs. To this end, descriptors such as volume fraction and size of nanofillers may need to be included in a physical-based viscoelastic model for modeling PNCs. Distinct from existing constitutive models for filled polymer, the new model will have all model parameters carrying physical significance and thus enable bottom-up material design of PNCs.

(iii) Advanced homogenization techniques of PNCs are desired, especially for nonlinear properties such as hyperelasticity. Existing DNS methods are accurate and flexible, but may be prohibited from design purpose due to the extremely high computational cost. On the other hand, most analytical micromechanics methods are limited to certain microstructure (e.g. spherical inclusions embedded in the matrix) and small strain assumption. A promising way is to enhance the homogenization with database precomputed by DNS methods as what has been done in SCA [115]. The challenging parts of data-driven approaches are always how to construct the database and how to extract data from the database efficiently.

(iv) It is necessary to study the mechanical behavior of emerging PNCs and their derivatives such as graphene-filled PNCs and nanocomposite hydrogels. Owing to their unprece-

dented mechanical, thermal and electrical properties, these new PNCs have wide applications such as sensors [116], electrodes, stimuli responsive devices [117], tissue scaffolds [118] and drug delivery agents [119]. Because of the new structural and physical characteristics of these PNCs (e.g. the high content of water in nanocomposite hydrogels), understanding the mechanical behavior of these new PNCs necessitates development of synergistically integrated modeling and high-fidelity experiments.

Finally, we note that tackling the above problems presents many challenges and opportunities for mechanicians and experimentalists. Hopefully, the synergistically integrated multiscale experiment and modeling will shed light on the understanding, design, and optimization of new PNCs by linking molecular level parameters to macroscopic material properties/performance.

Acknowledgments

References

1. Thomas A Vilgis, Gert Heinrich, and Manfred Klüppel. *Reinforcement of polymer nano-composites: theory, experiments and applications.* Cambridge University Press, 2009.

2. T Ramanathan, AA Abdala, S Stankovich, DA Dikin, M Herrera-Alonso, RD Piner, DH Adamson, HC Schniepp, X Chen, RS Ruoff, et al. Functionalized graphene sheets for polymer nanocomposites. *Nature nanotechnology*, 3(6):327–331, 2008.

3. T Ramanathan, H Liu, and LC Brinson. Functionalized swnt/polymer nanocomposites for dramatic property improvement. *Journal of Polymer Science Part B: Polymer Physics*, 43(17):2269–2279, 2005.

4. Ying Li, Martin Kröger, and Wing Kam Liu. Nanoparticle effect on the dynamics of polymer chains and their entanglement network. *Physical review letters*, 109(11):118001, 2012.

5. Ying Li, Martin Kröger, and Wing Kam Liu. Nanoparticle geometrical effect on structure, dynamics and anisotropic viscosity of polyethylene nanocomposites. *Macromolecules*, 45(4):2099–2112, 2012.

6. Ying Li, Martin Kröger, and Wing Kam Liu. Dynamic structure of unentangled polymer chains in the vicinity of non-attractive nanoparticles. *Soft Matter*, 10(11):1723–1737, 2014.

7. John A Moore, Ying Li, Devin T O'Connor, Wylie Stroberg, and Wing Kam Liu. Advancements in multiresolution analysis. *International Journal for Numerical Methods in Engineering*, 102(3-4):784–807, 2015.

8. M Steven Greene, Ying Li, Wei Chen, and Wing Kam Liu. The archetype-genome exemplar in molecular dynamics and continuum mechanics. *Computational Mechanics*, 53(4):687–737, 2014.

9. Meng-Jiao Wang. Effect of polymer-filler and filler-filler interactions on dynamic properties of filled vulcanizates. *Rubber Chemistry and Technology*, 71(3):520–589, 1998.

10. Albert Einstein. *Investigations on the Theory of the Brownian Movement.* Courier Corporation, 1956.

11. Hugh M Smallwood. Limiting law of the reinforcement of rubber. *Journal of applied physics*, 15(11):758–766, 1944.

12. SaFRJ Ahmed and FR Jones. A review of particulate reinforcement theories for polymer composites. *Journal of Materials Science*, 25(12):4933–4942, 1990.

13. Shao-Yun Fu, Xi-Qiao Feng, Bernd Lauke, and Yiu-Wing Mai. Effects of particle size, particle/matrix interface adhesion and particle loading on mechanical properties of particulate–polymer composites. *Composites Part B: Engineering*, 39(6):933–961, 2008.

14. DM Bigg. Mechanical properties of particulate filled polymers. *Polymer Composites*, 8(2):115–122, 1987.

15. RA Dickie. Heterogeneous polymer–polymer composites. i. theory of viscoelastic properties and equivalent mechanical models. *Journal of Applied Polymer Science*, 17(1):45–63, 1973.

16. Ioana C Finegan and Ronald F Gibson. Recent research on enhancement of damping in polymer composites. *Composite Structures*, 44(2):89–98, 1999.

17. K Li, X-L Gao, and AK Roy. Micromechanical modeling of viscoelastic properties of carbon nanotube-reinforced polymer composites. *Mechanics of Advanced Materials and Structures*, 13(4):317–328, 2006.

18. FT Fisher and LC Brinson. Viscoelastic interphases in polymer–matrix composites: theoretical models and finite-element analysis. *Composites Science and technology*, 61(5):731–748, 2001.

19. JS Bergström and MC Boyce. Constitutive modeling of the time-dependent and cyclic loading of elastomers and application to soft biological tissues. *Mechanics of materials*, 33(9):523–530, 2001.

20. JS Bergström and MC Boyce. Large strain time-dependent behavior of filled elastomers. *Mechanics of materials*, 32(11):627–644, 2000.

21. Jorgen S Bergstrom and Mary C Boyce. Mechanical behavior of particle filled elastomers. *Rubber chemistry and technology*, 72(4):633–656, 1999.

22. Hua Deng, Yu Liu, Donghai Gai, Dmitriy A Dikin, Karl W Putz, Wei Chen, L Catherine Brinson, Craig Burkhart, Mike Poldneff, Bing Jiang, et al. Utilizing real and statistically reconstructed microstructures for the viscoelastic modeling of polymer nanocomposites. *Composites Science and Technology*, 72(14):1725–1732, 2012.

23. Curt M Breneman, L Catherine Brinson, Linda S Schadler, Bharath Natarajan, Michael Krein, Ke Wu, Lisa Morkowchuk, Yang Li, Hua Deng, and Hongyi Xu. Stalking the materials genome: A data-driven approach to the virtual design of nanostructured polymers. *Advanced Functional Materials*, 23(46):5746–5752, 2013.

24. Yu Liu, M Steven Greene, Wei Chen, Dmitriy A Dikin, and Wing Kam Liu. Computational microstructure characterization and reconstruction for stochastic multiscale material design. *Computer-Aided Design*, 45(1):65–76, 2013.

25. Hongyi Xu, Yang Li, Catherine Brinson, and Wei Chen. A descriptor-based design methodology for developing heterogeneous microstructural materials system. *Journal of Mechanical Design*, 136(5):051007, 2014.

26. Hongyi Xu, Ruoqian Liu, Alok Choudhary, and Wei Chen. A machine learning-based design representation method for designing heterogeneous microstructures. *Journal of Mechanical Design*, 137(5):051403, 2015.

27. Aurélie Papon, Kay Saalwächter, Kerstin Schaler, Laurent Guy, François Lequeux, and Héléne Montes. Low-field nmr investigations of nanocomposites: Polymer dynamics and network effects. *Macromolecules*, 44(4):913–922, 2011.

28. Aurélie Papon, Héléne Montes, Mohamed Hanafi, François Lequeux, Laurent Guy, and Kay Saalwächter. Glass-transition temperature gradient in nanocomposites: evidence from nuclear magnetic resonance and differential scanning calorimetry. *Physical review letters*, 108(6):065702, 2012.

29. Francis W Starr, Thomas B Schrøder, and Sharon C Glotzer. Effects of a nanoscopic filler on the structure and dynamics of a simulated polymer melt and the relationship to ultrathin films. *Physical Review E*, 64(2):021802, 2001.

30. Francis W Starr, Thomas B Schrøder, and Sharon C Glotzer. Molecular dynamics simulation of a polymer melt with a nanoscopic particle. *Macromolecules*, 35(11):4481–4492, 2002.

31. Margarita Krutyeva, A Wischnewski, Michael Monkenbusch, Lutz Willner, Jon Maiz, Carmen Mijangos, Arantxa Arbe, J Colmenero, Aurel Radulescu, Olaf Holderer, et al. Effect of nanoconfinement on polymer dynamics: surface layers and interphases. *Physical review letters*, 110(10):108303, 2013.

32. T Glomann, GJ Schneider, J Allgaier, A Radulescu, W Lohstroh, B Farago, and D Richter. Microscopic dynamics of polyethylene glycol chains interacting with silica nanoparticles. *Physical review letters*, 110(17):178001, 2013.

33. Charles D Wood, Amin Ajdari, Craig Burkhart, Karl Putz, and L Catherine Brinson. Understanding competing mechanisms for glass transition changes in filled elastomers. *Composites Science and Technology*, 2016.

34. David S Simmons. An emerging unified view of dynamic interphases in polymers. *Macromolecular Chemistry and Physics*, 217(2):137–148, 2016.

35. Hua Liu and L Catherine Brinson. A hybrid numerical-analytical method for modeling the viscoelastic properties of polymer nanocomposites. *Journal of applied mechanics*, 73(5):758–768, 2006.

36. Zeliang Liu, John A Moore, Saad M Aldousari, Hassan S Hedia, Saeed A Asiri, and Wing Kam Liu. A statistical descriptor based volume-integral micromechanics model of heterogeneous material with arbitrary inclusion shape. *Computational Mechanics*, 55(5):963–981, 2015.

37. John A Moore, Ruizhe Ma, August G Domel, and Wing Kam Liu. An efficient multiscale model of damping properties for filled elastomers with complex microstructures. *Composites Part B: Engineering*, 62:262–270, 2014.

38. Yihu Song and Qiang Zheng. Application of two phase model to linear dynamic rheology of filled polymer melts. *Polymer*, 52(26):6173–6179, 2011.

39. Materials genome initiative. https://www.whitehouse.gov/mgi. Accessed: 2016-03-02.

40. K Hausler and MB Sayir. Nonlinear viscoelastic response of carbon black reinforced rubber derived from moderately large deformations in torsion. *Journal of the Mechanics and Physics of Solids*, 43(2):295–318, 1995.

41. John D Ferry. *Viscoelastic properties of polymers*. John Wiley & Sons, 1980.

42. Shan Tang, M Steven Greene, and Wing Kam Liu. Two-scale mechanism-based theory of nonlinear viscoelasticity. *Journal of the Mechanics and Physics of Solids*, 60(2):199–226, 2012.

43. Ying Li, Shan Tang, Brendan C Abberton, Martin Kröger, Craig Burkhart, Bing Jiang, George J Papakonstantopoulos, Mike Poldneff, and Wing Kam Liu. A predictive multiscale computational framework for viscoelastic properties of linear polymers. *Polymer*, 53(25):5935–5952, 2012.

44. Ying Li, Shan Tang, Martin Kröger, and Wing Kam Liu. Molecular simulation guided constitutive modeling on finite strain viscoelasticity of elastomers. *Journal of the Mechanics and Physics of Solids*, 88:204–226, 2016.

45. M Mooney. A theory of large elastic deformation. *Journal of applied physics*, 11(9):582–592, 1940.

46. RS Rivlin. Large elastic deformations of isotropic materials. iv. further developments of the general theory. *Philosophical Transactions of the Royal Society of London A: Mathematical, Physical and Engineering Sciences*, 241(835):379–397, 1948.

47. RW Ogden. Large deformation isotropic elasticity-on the correlation of theory and experiment for incompressible rubberlike solids. In *Proceedings of the Royal Society of London A: Mathematical, Physical and Engineering Sciences*, volume 326, pages 565–584. The Royal Society, 1972.

48. OH Yeoh. Some forms of the strain energy function for rubber. *Rubber Chemistry and technology*, 66(5):754–771, 1993.

49. AN Gent. A new constitutive relation for rubber. *Rubber chemistry and technology*, 69(1):59–61, 1996.

50. Gilles Marckmann and Erwan Verron. Comparison of hyperelastic models for rubber-like materials. *Rubber chemistry and technology*, 79(5):835–858, 2006.

51. LRG Treloar. The elasticity of a network of long-chain molecule-sii. *Transactions of the Faraday Society*, 39:241–246, 1943.

52. Werner Kuhn and F Grün. Beziehungen zwischen elastischen konstanten und dehnungsdoppelbrechung hochelastischer stoffe. *Kolloid-Zeitschrift*, 101(3):248–271, 1942.

53. Ellen M Arruda and Mary C Boyce. A three-dimensional constitutive model for the large stretch behavior of rubber elastic materials. *Journal of the Mechanics and Physics of Solids*, 41(2):389–412, 1993.

54. SF Edwards and Th Vilgis. The effect of entanglements in rubber elasticity. *Polymer*, 27(4):483–492, 1986.

55. M Kaliske and G Heinrich. An extended tube-model for rubber elasticity: statistical-mechanical theory and finite element implementation. *Rubber Chemistry and Technology*, 72(4):602–632, 1999.

56. C Miehe, S Göktepe, and F Lulei. A micro-macro approach to rubber-like materialspart i: the non-affine micro-sphere model of rubber elasticity. *Journal of the Mechanics and Physics of Solids*, 52(11):2617–2660, 2004.

57. Jacob D Davidson and NC Goulbourne. A nonaffine network model for elastomers undergoing finite deformations. *Journal of the Mechanics and Physics of Solids*, 61(8):1784–1797, 2013.

58. JC Simo. On a fully three-dimensional finite-strain viscoelastic damage model: formulation and computational aspects. *Computer methods in applied mechanics and engineering*, 60(2):153–173, 1987.

59. Sanjay Govindjee and Juan C Simo. Mullins effect and the strain amplitude dependence of the storage modulus. *International journal of solids and structures*, 29(14):1737–1751, 1992.

60. Alexander Lion. A constitutive model for carbon black filled rubber: experimental investigations and mathematical representation. *Continuum Mechanics and Thermodynamics*, 8(3):153–169, 1996.

61. J Lubliner. A model of rubber viscoelasticity. *Mechanics Research Communications*, 12(2):93–99, 1985.

62. J Keck and C Miehe. An eulerian overstress-type viscoplastic constitutive model in spectral form. formulation and numerical implementation. *Computational Plasticity; Fundamentals and Applications*, 1:997–1003, 1997.

63. Patrick Le Tallec, Christophe Rahier, and Ahmed Kaiss. Three-dimensional incompressible viscoelasticity in large strains: formulation and numerical approximation. *Computer methods in applied mechanics and engineering*, 109(3-4):233–258, 1993.

64. Sanjay Govindjee and Stefanie Reese. A presentation and comparison of two large deformation viscoelasticity models. *Journal of engineering materials and technology*, 119(3):251–255, 1997.

65. JS Bergström and MC Boyce. Constitutive modeling of the large strain time-dependent behavior of elastomers. *Journal of the Mechanics and Physics of Solids*, 46(5):931–954, 1998.

66. Christian Miehe and Serdar Göktepe. A micro–macro approach to rubber-like materials. part ii: the micro-sphere model of finite

rubber viscoelasticity. *Journal of the Mechanics and Physics of Solids*, 53(10):2231–2258, 2005.

67. M Doi and SF Edwards. The theory of polymer dynamics, volume 73 of international series of monographs on physics, 1986.

68. Ying Li, Brendan C Abberton, Martin Kröger, and Wing Kam Liu. Challenges in multiscale modeling of polymer dynamics. *Polymers*, 5(2):751–832, 2013.

69. Christopher J Ellison and John M Torkelson. The distribution of glass-transition temperatures in nanoscopically confined glass formers. *Nature Materials*, 2(10):695–700, 2003.

70. Perla Rittigstein, Rodney D Priestley, Linda J Broadbelt, and John M Torkelson. Model polymer nanocomposites provide an understanding of confinement effects in real nanocomposites. *Nature materials*, 6(4):278–282, 2007.

71. Xu Cheng, Karl W Putz, Charles D Wood, and L Catherine Brinson. Characterization of local elastic modulus in confined polymer films via afm indentation. *Macromolecular rapid communications*, 36:391–397, 2014.

72. Xu Cheng, Karl W Putz, Charles D Wood, and L Catherine Brinson. Characterization of local elastic modulus in confined polymer films via afm indentation. *Macromolecular rapid communications*, 36(4):391–397, 2015.

73. Supinda Watcharotone, Charles D Wood, Robert Friedrich, Xinqi Chen, Rui Qiao, Karl Putz, and L Catherine Brinson. Interfacial and substrate effects on local elastic properties of polymers using coupled experiments and modeling of nanoindentation. *Advanced Engineering Materials*, 13(5):400–404, 2011.

74. Bharath Natarajan, Yang Li, Hua Deng, L Catherine Brinson, and Linda S Schadler. Effect of interfacial energetics on dispersion and glass transition temperature in polymer nanocomposites. *Macromolecules*, 46(7):2833–2841, 2013.

75. Benjamin J Ash, Richard W Siegel, and Linda S Schadler. Glass-transition temperature behavior of alumina/pmma nanocomposites. *Journal of Polymer Science Part B: Polymer Physics*, 42(23):4371–4383, 2004.

76. Connie B Roth, Katie L McNerny, Wolter F Jager, and John M Torkelson. Eliminating the enhanced mobility at the free surface of polystyrene: fluorescence studies of the glass transition temperature in thin bilayer films of immiscible polymers. *Macromolecules*, 40(7):2568–2574, 2007.

77. Prince E Rouse Jr. A theory of the linear viscoelastic properties of dilute solutions of coiling polymers. *The Journal of Chemical Physics*, 21(7):1272–1280, 1953.

78. Pierre-Gilles De Gennes. *Scaling concepts in polymer physics*. Cornell university press, 1979.

79. TCB McLeish. Tube theory of entangled polymer dynamics. *Advances in physics*, 51(6):1379–1527, 2002.

80. Jagannathan T Kalathi, Gary S Grest, and Sanat K Kumar. Universal viscosity behavior of polymer nanocomposites. *Physical review letters*, 109(19):198301, 2012.

81. Jagannathan T Kalathi, Sanat K Kumar, Michael Rubinstein, and Gary S Grest. Rouse mode analysis of chain relaxation in polymer nanocomposites. *Soft matter*, 11(20):4123–4132, 2015.

82. Umi Yamamoto and Kenneth S Schweizer. Theory of entanglements and tube confinement in rod–sphere nanocomposites. *ACS Macro Letters*, 2(11):955–959, 2013.

83. Umi Yamamoto and Kenneth S Schweizer. Spatially dependent relative diffusion of nanoparticles in polymer melts. *The Journal of chemical physics*, 139(6):064907, 2013.

84. Klaus Nusser, Gerald J Schneider, and Dieter Richter. Rheology and anomalous flow properties of poly (ethylene-alt-propylene)–silica nanocomposites. *Macromolecules*, 46(15):6263–6272, 2013.

85. GJ Schneider, K Nusser, L Willner, P Falus, and D Richter. Dynamics of entangled chains in polymer nanocomposites. *Macromolecules*, 44(15):5857–5860, 2011.

86. Gerald J Schneider, Klaus Nusser, Susanne Neueder, Martin Brodeck, Lutz Willner, Bela Farago, Olaf Holderer, Wim J Briels, and Dieter Richter. Anomalous chain diffusion in unentangled model polymer nanocomposites. *Soft matter*, 9(16):4336–4348, 2013.

87. Brendan C Abberton, Wing Kam Liu, and Sinan Keten. Anisotropy of shear relaxation in confined thin films of unentangled polymer melts. *Macromolecules*, 48(20):7631–7639, 2015.

88. CLY Yeong and S Torquato. Reconstructing random media. ii. three-dimensional media from two-dimensional cuts. *Physical Review E*, 58(1):224, 1998.

89. Salvatore Torquato. *Random heterogeneous materials: microstructure and macroscopic properties*, volume 16. Springer Science & Business Media, 2013.

90. Veeraraghavan Sundararaghavan and Nicholas Zabaras. Classification and reconstruction of three-dimensional microstructures using support vector machines. *Computational Materials Science*, 32(2):223–239, 2005.

91. Aurélie Jean, Dominique Jeulin, Samuel Forest, Sabine Cantournet, and Franck NGUYEN. A multiscale microstructure model of carbon black distribution in rubber. *Journal of microscopy*, 241(3):243–260, 2011.

92. Lucien Laiarinandrasana, Aurélie Jean, Dominique Jeulin, and Samuel Forest. Modelling the effects of various contents of fillers on the relaxation rate of elastomers. *Materials & Design*, 33:75–82, 2012.

93. L Karasek and M Sumita. Characterization of dispersion state of filler and polymer-filler interactions in rubber-carbon black composites. *Journal of Materials Science*, 31(2):281–289, 1996.

94. Liang Chen, Weiming Zhou, Jie Lu, Jing Li, Wenhua Zhang, Ningdong Huang, Lihui Wu, and Liangbin Li. Unveiling reinforcement and toughening mechanism of filler network in natural rubber with synchrotron radiation x-ray nano-computed tomography. *Macromolecules*, 48(21):7923–7928, 2015.

95. RF Egerton, P Li, and M Malac. Radiation damage in the tem and sem. *Micron*, 35(6):399–409, 2004.

96. G Saheli, H Garmestani, and BL Adams. Microstructure design of a two phase composite using two-point correlation functions. *Journal of computer-aided materials design*, 11(2-3):103–115, 2004.

97. Anthony P Roberts. Statistical reconstruction of three-dimensional porous media from two-dimensional images. *Physical Review E*, 56(3):3203, 1997.

98. David Basanta, Mark A Miodownik, Elizabeth A Holm, and Peter J Bentley. Using genetic algorithms to evolve three-dimensional microstructures from two-dimensional micrographs. *Metallurgical and Materials Transactions A*, 36(7):1643–1652, 2005.

99. Ramin Bostanabad, Anh Tuan Bui, Wei Xie, Daniel W Apley, and Wei Chen. Stochastic microstructure characterization and reconstruction via supervised learning. *Acta Materialia*, 103:89–102, 2016.

100. Frédéric Feyel and Jean-Louis Chaboche. Fe 2 multiscale approach for modelling the elastoviscoplastic behaviour of long fibre sic/ti composite materials. *Computer methods in applied mechanics and engineering*, 183(3):309–330, 2000.

101. Ted Belytschko, Wing Kam Liu, Brian Moran, and Khalil Elkhodary. *Nonlinear finite elements for continua and structures*. John Wiley & Sons, 2013.

102. H. Moulinec and P. Suquet. A numerical method for computing the overall response of nonlinear composites with complex microstructure. *Computer Methods in Applied Mechanics and Engineering*, 157(12):69 – 94, 1998.

103. Rui Qiao and L Catherine Brinson. Simulation of interphase percolation and gradients in polymer nanocomposites. *Composites Science and Technology*, 69(3):491–499, 2009.

104. RD Peng, HW Zhou, HW Wang, and Leon Mishnaevsky. Modeling of nano-reinforced polymer composites: Microstructure effect on youngs modulus. *Computational Materials Science*, 60:19–31, 2012.
105. Xiaolei Yin, Wei Chen, Albert To, Cahal McVeigh, and Wing Kam Liu. Statistical volume element method for predicting microstructure–constitutive property relations. *Computer methods in applied mechanics and engineering*, 197(43):3516–3529, 2008.
106. Hal F Brinson and L Catherine Brinson. *Polymer engineering science and viscoelasticity: an introduction*. Springer Science & Business Media, 2007.
107. Zvi Hashin. The elastic moduli of heterogeneous materials. *Journal of Applied Mechanics*, 29(1):143–150, 1962.
108. Zvi Hashin and S Shtrikman. A variational approach to the theory of the elastic behaviour of multiphase materials. *Journal of the Mechanics and Physics of Solids*, 11(2):127–140, 1963.
109. Salvatore Torquato. Random heterogeneous media: microstructure and improved bounds on effective properties. *Applied mechanics reviews*, 44(2):37–76, 1991.
110. JOHN D Eshelby. The determination of the elastic field of an ellipsoidal inclusion, and related problems. In *Proceedings of the Royal Society of London A: Mathematical, Physical and Engineering Sciences*, volume 241, pages 376–396. The Royal Society, 1957.
111. T Mori and K Tanaka. Average stress in matrix and average elastic energy of materials with misfitting inclusions. *Acta metallurgica*, 21(5):571–574, 1973.
112. R1 Hill. A self-consistent mechanics of composite materials. *Journal of the Mechanics and Physics of Solids*, 13(4):213–222, 1965.
113. Hua Liu and L Catherine Brinson. Reinforcing efficiency of nanoparticles: a simple comparison for polymer nanocomposites. *Composites Science and Technology*, 68(6):1502–1512, 2008.
114. Julie Diani, Pierre Gilormini, Yannick Merckel, and Fabien Vion-Loisel. Micromechanical modeling of the linear viscoelasticity of carbon-black filled styrene butadiene rubbers: The role of the filler–rubber interphase. *Mechanics of Materials*, 59:65–72, 2013.
115. Zeliang Liu, A. Miguel Bessa, and Wing Kam Liu. Self-consistent clustering analysis: an efficient multi-scale scheme for inelastic heterogeneous materials. *Computer Methods in Applied Mechanics and Engineering*, 2016.
116. Ling Chen, GH Chen, and Liang Lu. Piezoresistive behavior study on finger-sensing silicone rubber/graphite nanosheet nanocomposites. *Advanced Functional Materials*, 17(6):898–904, 2007.
117. Xingcheng Xiao, Tao Xie, and Yang-Tse Cheng. Self-healable graphene polymer composites. *Journal of Materials Chemistry*, 20(17):3508–3514, 2010.
118. Shengbing Yang, Jing Wang, Honglue Tan, Fanyan Zeng, and Changsheng Liu. Mechanically robust pegda–msns-oh nanocomposite hydrogel with hierarchical meso-macroporous structure for tissue engineering. *Soft Matter*, 8(34):8981–8989, 2012.
119. Mohamadreza Nassajian Moghadam, Vitaliy Kolesov, Arne Vogel, Harm-Anton Klok, and Dominique P Pioletti. Controlled release from a mechanically-stimulated thermosensitive self-heating composite hydrogel. *Biomaterials*, 35(1):450–455, 2014.